

## Magnetocrystalline Anisotropy of Pure and Doped Hematite\*

P. J. BESSER,<sup>†</sup> A. H. MORRISH,<sup>‡</sup> AND C. W. SEARLE<sup>‡</sup>

*University of Minnesota, Minneapolis, Minnesota*

(Received 22 June 1966)

The magnetocrystalline anisotropy of synthetic single crystals of hematite ( $\alpha$ -Fe<sub>2</sub>O<sub>3</sub>), both pure and doped with Ga<sup>3+</sup>, Al<sup>3+</sup>, and Ti<sup>4+</sup>, has been measured. The principal anisotropy constant  $K_1'$  has been determined below the low-temperature (Morin) transition by spin-flop measurements. An analysis of these data that considers the origins of the anisotropy has permitted the prediction of the transition temperature. Although the transition temperature is a sensitive function of doping, the predicted values are in excellent agreement with those observed experimentally. The magnetocrystalline anisotropy in the basal plane above the transition temperature has been studied with ferromagnetic-resonance techniques. The in-plane anisotropy is observed to be remarkably sensitive to stress but only slightly dependent on doping.

### INTRODUCTION

HEMATITE is the iron sesquioxide that crystallizes into the structure with space group  $R\bar{3}c$  (full symbol  $R\bar{3}2/c$ , Schoenflies symbol  $D_{3d}^6$ ). If rhombohedral axes of reference are chosen to describe this trigonal system, the iron ions lie along the [111] axis with spins ordered in the sequence  $+-+$  below the Néel temperature  $T_N (=948^\circ\text{K})$ . Layers of oxygen ions lying perpendicular to the trigonal axis alternate with similarly oriented layers of iron ions. In a cation layer, half the iron ions lie 0.30 Å above and the other half an equal distance below the layer's medial plane. Although the over-all magnetic structure is antiferromagnetic, the magnetic moments of the iron ions within one (111) layer are arranged ferromagnetically.

This paper reports on a study of the magnetocrystalline anisotropy of pure and doped hematite single crystals. From the crystal symmetry it follows that this anisotropy can be described in general by a free-energy expression of the form<sup>1</sup>

$$F_K = K_1' \sin^2\theta + K_2' \sin^4\theta + K_3' \sin^6\theta + K_3'' \sin^6\theta \cos 6\varphi. \quad (1)$$

Here  $K_1'$ ,  $K_2'$ ,  $K_3'$ , and  $K_3''$  are anisotropy constants that depend on temperature,  $\theta$  is the angle between the magnetization of one sublattice and the [111] axis, and  $\varphi$  is the azimuthal angle, that is, the angle between the component of a sublattice's magnetization and a suitably chosen reference direction in the (111) plane. Equation (1) assumes that the angles made by the magnetizations of the two sublattices with the reference direction differ by  $\pi$  radians; this is a reasonable approximation for an antiferromagnet.

Now, in addition to the paramagnetic-antiferromagnetic transition at the Néel temperature, hematite usually undergoes a magnetic transformation, often called the Morin transition, at a much lower tempera-

ture; for pure hematite this transition occurs at  $T \approx 263^\circ\text{K}$ . At temperatures below the lower transition, the spins lie either along or almost along the trigonal axis. Neutron diffraction<sup>2,3</sup> and other experiments<sup>4</sup> indicate that the spins may be canted at an angle of  $\theta \approx 5^\circ$  with respect to the [111] direction. If so, at least two anisotropy constants  $K_1'$  and  $K_2'$  are required to describe the anisotropy in this temperature region.<sup>2</sup> However, the interpretation of the data is not unambiguous. For the present purposes, it is simpler to assume that the spins are exactly aligned along the [111] axis since then only one anisotropy constant  $K_1'$  is needed. We have determined  $K_1'$  for the low-temperature structure of hematite as a function of temperature and doping by means of spin-flop measurements.

For temperatures between the Morin transition and Néel temperatures, the atomic magnetic moments lie in the basal plane. Thus,  $K_1'$  is positive below the lower transition and negative above it. The two main sources of the magnetocrystalline anisotropy of hematite are believed to be the magnetic-dipole and single-ion anisotropies.<sup>5</sup> A calculation of the dipolar anisotropy<sup>5</sup> together with the spin-flop data has permitted the temperature at which  $K_1'$  changes sign to be predicted as a function of doping. These temperatures are compared with those determined experimentally for the Morin transition from magnetization, magnetic resonance, and neutron-diffraction observations. The neutron-diffraction measurements have already been published<sup>6</sup>; the other experimental data are presented here for the first time.

When the spins lie in the (111) plane, the magnetocrystalline-anisotropy energy expression reduces to

$$F_K = K(T) + K_3'' \cos 6\varphi. \quad (2)$$

We did not have the means of evaluating  $K(T)$  at our disposal. Because the in-plane anisotropy constant  $K_3''$

<sup>2</sup> A. H. Morrish, G. B. Johnston, and N. A. Curry, *Phys. Letters* **7**, 177 (1963).

<sup>3</sup> R. Nathans, S. J. Pickart, H. A. Alperin, and P. J. Brown, *Phys. Rev.* **136**, A1641 (1964).

<sup>4</sup> S. Foner and S. J. Williamson, *J. Appl. Phys.* **36**, 1154 (1965).

<sup>5</sup> J. O. Artman, J. C. Murphy, and S. Foner, *Phys. Rev.* **138**, A912 (1965).

<sup>6</sup> N. A. Curry, G. B. Johnston, P. J. Besser, and A. H. Morrish, *Phil. Mag.* **12**, 221 (1965).

\* This research was supported by the National Science Foundation under Grant No. G18990.

<sup>†</sup> Present address: Autonetics Division of North American Aviation, Anaheim, California.

<sup>‡</sup> Present address: University of Manitoba, Winnipeg, Canada.

<sup>1</sup> A. H. Morrish, *The Physical Principles of Magnetism* (John Wiley & Sons, Inc., New York, 1965), p. 470.

is small, its measurement by static methods is very difficult. We have employed microwave-resonance techniques, since fortunately it turns out that  $K_3''$  can be conveniently determined by this method. Briefly, the reason is as follows: Hematite possesses a small spontaneous magnetization lying in the (111) plane, because the two ferric sublattices are canted slightly as a result of the Dzialoshinski-Moriya interaction.<sup>7</sup> One of the resonance modes corresponds roughly to a precession of the weak moment about its equilibrium position and can be observed with microwaves of centimeter wavelength. The term involving  $K_3''$  in the resonance condition for this low-frequency mode is multiplied by the molecular field,<sup>8</sup> which is a large ( $\approx 10^7$  Oe for hematite) quantity. This magnifying action makes the in-plane anisotropy comparatively easy to observe.

### SPIN-FLOPPING EXPERIMENTS

Highly perfect single crystals of hematite were grown by procedures described elsewhere.<sup>6</sup> Some of the crystals were doped with small amounts of either  $\text{Ga}^{3+}$ ,  $\text{Al}^{3+}$ , or  $\text{Ti}^{4+}$  ions. The actual amount of doping was determined by x-ray fluoroscopy for Ga and Ti and by wet-chemical analysis for Al.

A spin-flop transition is a field-induced one in which the sublattice magnetizations of a uniaxial antiferromagnet are decoupled from the crystal's easy axis and rotated into the plane perpendicular to this axis by application of a field parallel to the easy axis. The critical field required to produce spin flopping  $H_{st}$  is given, under certain assumptions, by

$$H_{st} = (2H_m H_{K_1'})^{1/2}, \quad (3)$$

where

$$H_{K_1'} = K_1'/M.$$

Here  $H_m$  is the exchange or molecular field,  $H_{K_1'}$  is the equivalent anisotropy field, and  $M$  is the magnetization of one sublattice. It follows that, for hematite,  $H_{st}$  is likely to be large.

The requisite applied fields were produced by a pulse method. A capacitor bank of  $10^3 \mu\text{F}$  that could be charged to a maximum of  $3 \times 10^3$  V was discharged through a small low-resistance solenoid. The field coil was 3.87 in. long, 1.035 in. in mean diam, and wound on a plastic tube of  $\frac{3}{8}$ -in. i.d. The coil was immersed in liquid nitrogen for cooling purposes and to lower its resistance by a factor of about 7. The measured value of the maximum field was 120 000 Oe.

The spin flop was detected by displaying  $M$ - $H$  loops on an oscilloscope. This display was accomplished by means of a pair of pickup coils each  $\frac{1}{2}$  in. in length and wound in series opposition on a 6-mm-i.d. Pyrex tube. With no sample present, the coils were balanced for zero

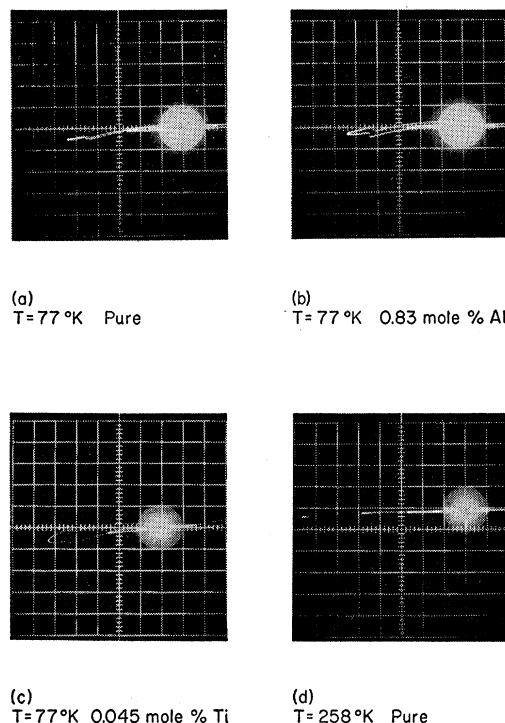


FIG. 1. Spin-flop transitions in pure and doped hematite crystals. (a)  $H_{st} = 67.8$  kOe, (b)  $H_{st} = 64.0$  kOe, (c)  $H_{st} = 64.6$  kOe, and (d)  $H_{st} = 26.2$  kOe.

output when the drive-field flux changed. Insertion of a sample into one of the coils, called the  $M$  coil, produced an output voltage from the differential coil arrangement that was proportional to the magnetization  $M$  of the sample. The other coil, called the  $H$  coil, yielded an output proportional to the drive field  $H$ . The horizontal scale of the oscilloscope was calibrated in terms of the drive field  $H$  with the aid of gaussmeter and output-voltage measurements and confirmed with calculations.

In order to arrange that the spin-flop transition occurs over as narrow a range of drive field as possible, it is imperative that the easy axis be aligned nearly parallel to the direction of the applied field. First the hematite crystal was oriented by x-ray methods and cut into disks with faces that were within  $1^\circ$  of being (111) planes. A (111) face of each sample was next glued with epoxy resin on the end of a nylon cylinder so machined that, upon insertion into the Pyrex tube, the crystal was firmly positioned at the center of the  $M$  coil. The pickup and sample assembly were then put into a Dewar which, in turn, was placed inside the drive coil. These fits were quite snug and hence ensured that the crystal and sensing-coil axes would be parallel to that of the drive coil. Liquid nitrogen was used as the coolant in the inner Dewar. After the  $\text{N}_2$  had boiled away, the warmup of the sample was slow enough to permit the spin-flop field to be determined as a function of temperature.

<sup>7</sup> I. Dzialoshinski, Zh. Eksperim. i Teor. Fiz. 33, 1454 (1959) [English transl.: Soviet Phys.—JETP 6, 1120 (1958)]; T. Moriya, Phys. Rev. 120, 91 (1960).

<sup>8</sup> P. Pincus, Phys. Rev. Letters 5, 13 (1960).

TABLE I. Data on pure and doped hematite.

Foreign cation	Mole % (measured)	$H_{sf}$ (kOe) $T=77^\circ\text{K}$	$H_{K1}$ (Oe) $T=0^\circ\text{K}$	Transition temperature ( $^\circ\text{K}$ )			
				Theor.	Magnet.	Neut. diff.	Reson.
Pure	...	$67.8 \pm 3.4$	217	266	263	263	263
Al <sup>3+</sup>	0.42	66.2	207	264	258	258	...
Al <sup>3+</sup>	0.83	64.0	193	256	255	256	...
Al <sup>3+</sup>	1.28	62.2	182	251	252	252	252
Al <sup>3+</sup>	$\sim 1.5$	57.5	157	246	242	254	...
Ga <sup>3+</sup>	0.30	65.5	206	264	258	258	257
Ga <sup>3+</sup>	0.60	63.0	187	255	253	251	252
Ga <sup>3+</sup>	1.38	57.5	156	245	241	243	243
Ti <sup>4+</sup>	0.045	64.6	197	260	259	264	252
Ti <sup>4+</sup>	0.085	56.6	151	243	243	253	239
Ti <sup>4+</sup>	0.170	...	...	...	206	246	...
Ti <sup>4+</sup>	0.258	...	...	...	<77	<12	...
Ti <sup>4+</sup>	0.383	...	...	...	<77	<12	...

The temperature of the sample was measured with a thermocouple inserted inside the Pyrex coil form and making contact with the hematite crystal.

The  $M$ - $H$  loop displayed on the oscilloscope was photographed with a Polaroid C-12 camera. Typical photographs are shown in Fig. 1. Since the camera shutter was operated manually, a large white spot from the halo around the electron beam occurs in the print. Only the positive swings of the trace representing the alternating  $H$  field are shown, because the beam spot has been moved to the right of the screen in order to increase the accuracy in the measurement of  $H_{sf}$ . As the critical field is reached, a sudden increase in  $M$  occurs; a corresponding decrease occurs after the field has reached its maximum and returned to lower values. It is apparent from Fig. 1 that there appears to be a hysteresis in the spin flop. We did not investigate whether all the hysteresis was due to the electronics of the measurement circuitry or whether part was a true hysteresis in the transition. The critical field was taken to be the value at which the flop occurred for increasing

$H$ . This value was found to be independent of the maximum applied field, whereas the field at which the spins fell back to the easy direction appeared to be field-dependent. Because of amplifier drift and imbalance in the sensing coils, the electron beam did not always travel along the  $x$  axis of the graticule. As a consequence, the positions of the  $H=0$  and  $H=H_{sf}$  points were extended vertically to the  $x$  axis of the graticule, and all measurements were made along this axis for consistency. It is estimated that this method led to  $H_{sf}$  values accurate to about 5%.

The spin-flop transition was very sharp for pure, Al-doped, and Ga-doped hematite, whereas for Ti-doped crystals the increase in  $M$  was more gradual. This feature is illustrated by Figs. 1(a), 1(b), and 1(c), which show the  $M$ - $H$  characteristic at  $77^\circ\text{K}$  for pure, 0.83 mole % Al-doped samples, and 0.045 mole % Ti-doped samples, respectively. The transition for this Ti-doped crystal occurred over a field range of 5 kOe; for higher Ti content, the transition was even more gradual, until for a sample with 0.17 mole % Ti no spin flopping was detected. A possible explanation will be advanced later. The values of  $H_{sf}$  chosen for those Ti-doped samples exhibiting spin flop corresponded to the midpoint of the magnetization increase.

The spin-flop signal becomes weaker as the temperature approaches the Morin transition point, as shown for a pure sample at  $T=258^\circ\text{K}$  in Fig. 1(d). As a result, it was not possible to make measurements close to the transition temperature. The spin-flop field is plotted as a function of temperature for one pure and three doped hematite crystals in Fig. 2. It is to be noted that the temperature dependence is roughly the same for samples with different types and amounts of impurities present. The spin-flop fields at  $T=77^\circ\text{K}$  for a systematic series of dopings are listed in Table I. These data appear to be consistent with the recently reported values of  $65 \pm 3$  kOe<sup>9</sup> and  $67.8 \pm 3.4$  kOe<sup>10</sup> obtained for a natural, but

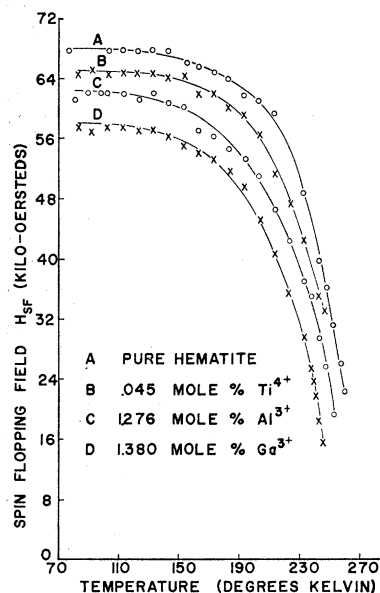


FIG. 2. Temperature dependence of the spin-flop field for some synthetic single crystals of hematite with various dopings.

<sup>9</sup> S. Foner, in *Proceedings of the International Conference on Magnetism, Nottingham, 1964* (Institute of Physics and the Physical Society, London, 1964), p. 438.

<sup>10</sup> N. Blum, A. J. Freeman, J. W. Shaner, and L. Grodzins, *J. Appl. Phys.* **36**, 1169 (1965).

presumably relatively pure, crystal from Elba. From Table I, it can be seen that at  $T=77^\circ\text{K}$  the spin-flop field decreases linearly with impurity content for Al- and Ga-doped crystals and almost linearly for the Ti-doped crystals.<sup>11</sup>

Equation (3) is valid, provided that  $\chi_{\parallel} \ll \chi_{\perp}$ , where  $\chi_{\parallel}$  and  $\chi_{\perp}$  are the susceptibilities measured parallel and perpendicular to the  $[111]$  axis, respectively, and that  $H_{sf} \gg H_D$ , where  $H_D$  is the Dzialoshinski-Moriya equivalent field. In addition, certain terms tentatively proposed by Foner<sup>9</sup> have been omitted. The conditions under which Eq. (3) holds are best met at low temperatures.

From Fig. 2, it is apparent that the spin-flop field is almost constant from 130 to  $77^\circ\text{K}$ ; in addition, Foner has found<sup>9</sup> that, for a natural crystal,  $H_{sf}$  is constant from 77 to  $4^\circ\text{K}$ . We will therefore assume that the spin-flop field remains constant from  $77^\circ\text{K}$  to absolute zero for all the specimens; for pure hematite, then,  $H_{sf} = 67.8$  kOe at  $T=0^\circ\text{K}$ . It is to be recalled that  $H_m = N_{AB}M$  and  $N_{AB} = 1/\chi_{\perp}$ , where  $N_{AB}$  is the molecular-field constant and  $M$  is the magnetization of one ferric sublattice. By taking<sup>12</sup>  $N_{AB} = 1.15 \times 10^4$  and  $M = 920$  emu/cm<sup>3</sup>, Eq. (3) yields  $H_{K_1'} = 217$  Oe for pure hematite at absolute zero. Table I also lists the calculated values of  $H_{K_1'}$  for the doped crystals.

### PREDICTION OF THE TRANSITION TEMPERATURE

The magnetocrystalline anisotropy is believed to have in general three main microscopic sources, namely: (1) the magnetic-dipolar anisotropy  $K_{md}$ , (2) the single-ion anisotropy  $K_{si}$ , and (3) the exchange anisotropy  $K_e$ . The third of these,  $K_e$ , which is given approximately by  $K_{si}(kT_N/\Delta E_{cf})$ , where  $\Delta E_{cf}$  is the splitting of the lowest orbital levels by the crystalline field, is probably negligibly small compared to  $K_{md}$  and  $K_{si}$ .

The dipolar anisotropy has its origin simply in the interaction of the magnetic moments of the individual ions. This anisotropy energy depends on the geometrical and orientational configuration of the moments. The value of  $K_{md}$  obtained from the summation computation is quoted by Tachiki and Nagamiya<sup>13</sup> to be  $-1.15$  cm<sup>-1</sup>/ion at  $T=0^\circ\text{K}$ , and is found by Artman *et al.*<sup>5</sup> to be  $-1.172$  cm<sup>-1</sup>/ion. The equivalent dipolar anisotropy field corresponding to the latter value is  $H_{md} = -100.4 \times 10^2$  Oe. The negative sign of course implies that the spin direction favored lies in the basal plane.

It is not practical at this time to make a calculation of the single-ion anisotropy. Instead, by following the approach of Artman *et al.*,<sup>5</sup> a value for the equivalent single-ion anisotropy field can be obtained from the experimental anisotropy constant  $H_{K_1'}$  via the relation-

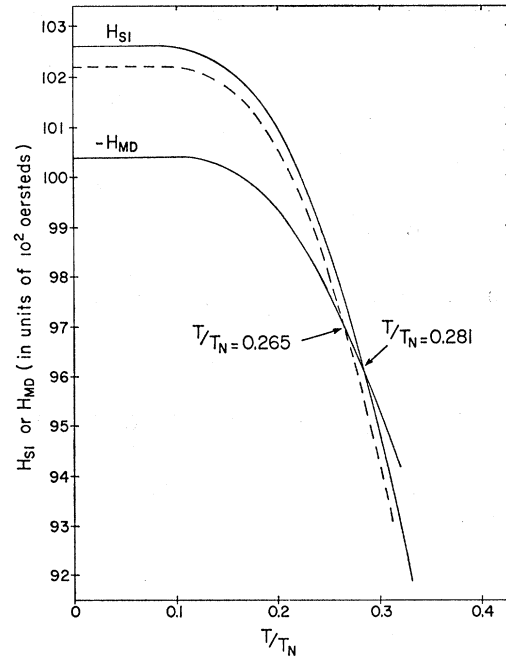


Fig. 3. The equivalent magnetic-dipole ( $H_{md}$ ) and single-ion ( $H_{si}$ ) anisotropy fields of  $\alpha\text{-Fe}_2\text{O}_3$  plotted as a function of temperature. The full curve for  $H_{si}$  is for pure hematite and the dashed one is for hematite doped with 1.28 mole % Al.

ship  $H_{si} = H_{K_1'} - H_{md}$ ; from our data,  $H_{si} = 102.6 \times 10^2$  Oe for pure hematite at absolute zero. Thus,  $H_{md}$  and  $H_{si}$  have opposite signs and differ by only 2% in magnitude.

The temperature dependences expected for the anisotropy constants have been calculated on the basis of the molecular-field approximation.<sup>14</sup> The dipolar anisotropy is given by

$$H_{md}(T) = H_{md}(0)B_S^2(z), \quad (4)$$

where

$$\begin{aligned} z &= (g\mu_B S/kT)N_{AB}M \\ &= (Ng^2\mu_B^2 S^2/2kT)B_S(z). \end{aligned} \quad (5)$$

Here,  $B_S(z)$  is the Brillouin function for spin quantum number  $S (= \frac{5}{2})$ ,  $N$  is the number of ferric ions per unit volume,  $\mu_B$  is the Bohr magneton, and  $g$  is the splitting factor for the  $\text{Fe}^{3+}$  ions. On the other hand, the variation of the single-ion anisotropy with temperature is found to be

$$H_{si}(T) = H_{si}(0)[2(S+1) - 3B_S(z) \coth(z/2S)]. \quad (6)$$

Both  $H_{md}(0)$  and  $H_{si}(0)$  contain  $N$  and  $S$  as factors. The magnitudes of the anisotropy fields predicted by Eqs. (4) and (6) for pure  $\alpha\text{-Fe}_2\text{O}_3$  are plotted in Fig. 3. Because of the difference in the temperature variations, the two curves intersect at  $T = 0.281T_N$  or  $266^\circ\text{K}$ . As Artman *et al.*<sup>5</sup> have already pointed out, this tempera-

<sup>11</sup> P. J. Besser and A. H. Morrish, *Phys. Letters* **13**, 289 (1964).

<sup>12</sup> C. Guillaud, *J. Phys. Radium* **12**, 489 (1951).

<sup>13</sup> M. Tachiki and T. Nagamiya, *J. Phys. Soc. Japan* **13**, 452 (1958).

<sup>14</sup> K. Yoshida, *Progr. Theoret. Phys. (Kyoto)* **6**, 691 (1951); M. Tachiki and T. Nagamiya, *J. Phys. Soc. Japan* **13**, 452 (1958).

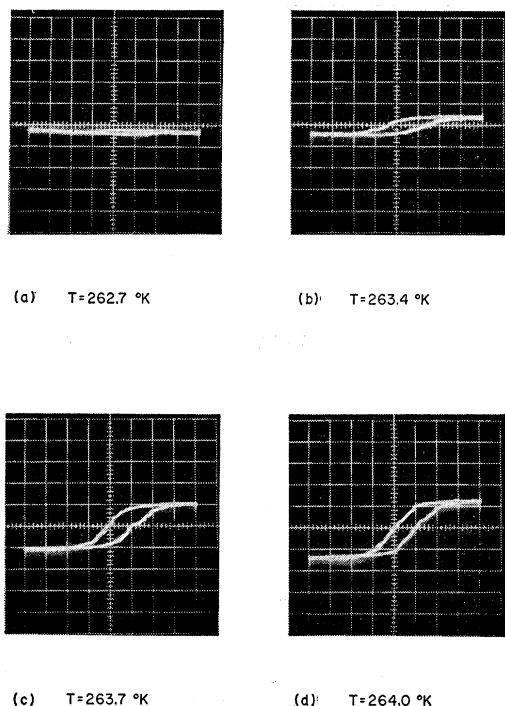


FIG. 4. The low-temperature (Morin) transition for pure hematite detected via the temperature variation of the  $M$ - $H$  loop of the weak ferromagnetic moment.

ture agrees well with that observed for the Morin transition (263°K).

The transition temperatures expected for the doped crystals can be obtained in a similar way. For example, consider the sample doped with 1.28 mole % Al. Since  $H_{K_1}(0) = 182$  Oe, it follows that  $H_{si}(0) = 102.2 \times 10^3$  Oe if  $H_{md}(0)$  is unchanged. The temperature dependence of the single-ion anisotropy field for this value of  $H_{si}(0)$  is also shown in Fig. 3. The intersection with the  $H_{md}$  curve then yields  $T = 0.265T_N$  or 251°K for the transition temperature. This procedure was carried out for all the doped samples on which spin-flop data had been taken; these theoretical transition temperatures are listed in Table I.

In the foregoing analysis, it was assumed that  $H_{md}$  was independent of doping. Actually, the substitution of impurities will, in general, affect both anisotropies. Any shift that may occur in  $H_{md}(0)$  will not, however, change the transition temperature obtained from the graphical procedure. This follows, since the crossover temperature of the two curves depends on the difference between the low-temperature magnitudes and not on their absolute values. The introduction of  $Ti^{4+}$  ions into the lattice substitutionally produces a more complicated situation than the introduction of either  $Ga^{3+}$  or  $Al^{3+}$  ions, since, in the former case, charge balance requires the presence of an equal number of  $Fe^{2+}$  ions. Then not only the magnitudes but also the temperature dependences of the two anisotropy fields are changed. In order

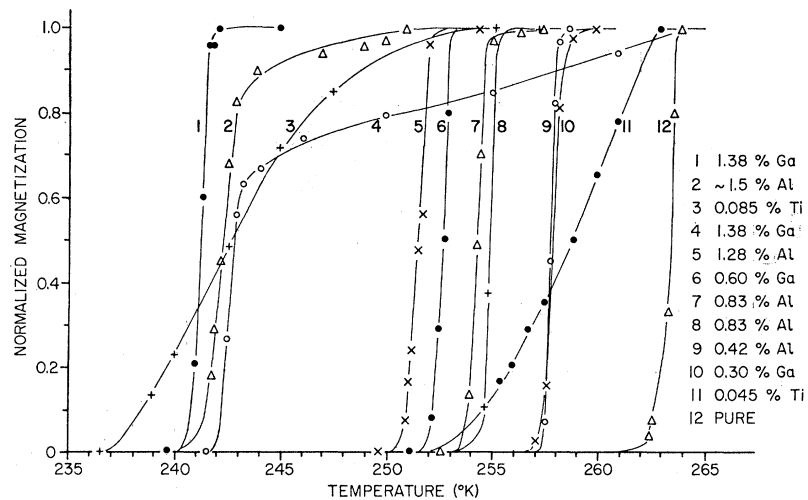
to calculate the temperature variation it is necessary to know the  $g$  value and the molecular field for the ferrous ions. Although a recent model in which the ferrous ions are treated as a third sublattice leads to an estimate of these quantities,<sup>15</sup> they cannot be considered to be known at present. However, the highest doped sample for which spin flopping was observed contained only 0.085 mole % Ti. It is reasonable to suppose that the contribution of such a small number of ferrous ions to the temperature dependence of  $H_{md}$  and  $H_{si}$  would be able to shift the intersection of the two curves by at most a few degrees. Again, it is the relative and not the absolute changes in the magnitudes of  $H_{md}(0)$  and  $H_{si}(0)$  that affect the predicted transition temperature.

Clearly, the reason the transition temperature is very sensitive to small amounts of impurities is the near equality in the magnitudes of  $H_{md}$  and  $H_{si}$ . In order to completely inhibit the transition, it is only necessary that the difference  $H_{si} - |H_{md}|$  be reduced from 217 to 0 Oe. It is of interest to explore the mechanisms whereby the different impurity ions affect the anisotropy. The substitution of a diamagnetic ion with an ionic radius different from that of a ferric ion will lead to a lattice distortion in the vicinity of the impurity. The shift in position of the anions surrounding the diamagnetic ion will also affect the crystalline field at the neighboring magnetic cations. Since the ground state of the ferric ions is an  $S$  state, the spin-orbit interaction enters only in higher order. Hence, substitution of  $Al^{3+}$  or  $Ga^{3+}$  will produce an effect on the single-ion anisotropy of the neighboring ferric ions only to higher order. On the other hand, the ferrous ions present with  $Ti^{4+}$  doping are in a  $D$  ground state and are influenced much more strongly by the crystalline field, since the spin-orbit interaction is of first order. Further, the ionic radius of a ferrous ion is 0.74 Å, compared to 0.64 Å for a ferric ion, and therefore additional lattice distortion will be produced. To summarize, superposed on the lattice distortion from Ti ions, there are stronger spin-orbit coupling, larger ionic radius, and different anisotropy temperature dependence of the ferrous ions. As a consequence, it is to be expected that  $Ti^{4+}$  doping will have a greater effect on the single-ion anisotropy than either  $Al^{3+}$  or  $Ga^{3+}$ .

The source of the difference between the Al and Ga dopings is not so easily discerned. Both are nonmagnetic ions with smaller ionic radii than the  $Fe^{3+}$  ion. The radius of  $Ga^{3+}$  is almost the same as the  $Fe^{3+}$  radius, but that of the  $Al^{3+}$  ion is about 10% smaller. On this basis alone, one would anticipate that gallium would cause less distortion of the lattice than the aluminum. That the reverse is true may be due to crystal-structure effects.  $Al_2O_3$  and  $\alpha$ - $Fe_2O_3$  are isomorphous, and solid solutions of mixed crystals show no change in crystal structure in the system  $Al_{2-x}Fe_xO_3$  throughout the

<sup>15</sup> C. W. Searle and A. H. Morrish, J. Appl. Phys. 37, 1141 (1966).

Fig. 5. The spontaneous magnetization of pure and doped hematite crystals as a function of temperature. The magnetization is normalized to the room-temperature value.



entire range of  $x$  from 0 to 2. The compound  $\text{GaFeO}_3$ , however, has a different crystal structure than hematite, and the tendency to distort from the hematite structure may be present even at low levels of gallium doping. Incidentally,  $\text{FeTiO}_3$  (ilmenite) has the same crystal structure as hematite.

The linearity of  $H_{K_1}$  versus impurity content is somewhat anticipated, since many physical, and in particular magnetic, phenomena follow a linear approximation for low values of the perturbing mechanism. The dipole anisotropy would be expected to vary linearly with  $n$ , the impurity %, for low dopings, viz.,

$$H_{\text{md}}(n) = H_{\text{md}}(0)(1-n), \quad (7)$$

since each impurity removes one ionic dipole from the interaction. If the single-ion anisotropy varies because of the change in the crystalline field acting via the spin-orbit coupling of the magnetic neighbors of the impurity, then  $H_{\text{si}}$  will be proportional to the product of the doping level  $n$  and the effective number of magnetic neighbors  $z$  at low impurity concentrations, viz.,

$$H_{\text{si}}(n) = H_{\text{si}}(0)(1-zn). \quad (8)$$

Obviously, the total anisotropy will also vary linearly, since it is the difference of two linear variations. If Eqs. (7) and (8) are correct, it is also clear that  $H_{\text{si}}$  will decrease more rapidly with impurity content than  $H_{\text{md}}$ . Hence, at heavy enough doping levels,  $H_{\text{si}}$  may become less than  $H_{\text{md}}$  even at  $T=0^\circ\text{K}$ ; presumably this is what happens in the samples most heavily doped with Ti.

#### MEASUREMENTS OF THE TRANSITION TEMPERATURE

In comparing the theoretical transition temperature with experimental values, it is particularly pertinent to perform the measurements on the same crystals used in the spin-flop experiments. This was easily achieved

with basically the same equipment employed for the critical-field determinations, except now the field coil was driven by a steady 60-cps sinusoidal source. The  $M$ - $H$  loop associated with the weak ferromagnetic moment of the sample was observed by taking the  $H$  signal directly from the field coil and by using a larger amplification for the  $M$  signal. When the easy axis for the spin directions changes from the (111) plane to the [111] direction, the small spontaneous magnetization virtually disappears. Hence, the transition region can be determined by observing the magnitude of this magnetization as a function of temperature.

For the present measurements, the samples were rotated by  $90^\circ$  from their previous orientation, that is, the drive field now was applied in the basal plane. Since the temperature range over which the transition occurs often is only about  $1^\circ\text{C}$ , it was necessary to vary the temperature slowly enough to permit several Polaroid pictures to be taken in the transition region. This was achieved by cooling the sample either with methanol and dry ice or with Freon-11 and liquid nitrogen to a temperature where  $M=0$ , and then allowing the system to warm up slowly. The warming rate obtained was  $\frac{1}{4}$ - $\frac{1}{2}^\circ\text{C}$  per minute, depending on the temperature. Typical photographs for a pure hematite crystal are shown in Fig. 4 and illustrate the sharpness of the transition.

The magnetization relative to the room-temperature values was determined as a function of temperature from the prints; several  $M$ -versus- $T$  curves are plotted in Fig. 5. Curves 7 and 8 are for samples each containing 0.83% Al, but grown in different runs; the relative shift between these two curves is everywhere less than  $1^\circ\text{C}$ . On the other hand, the difference between Curves 1 and 4, both for samples doped with 1.38% Ga, is much greater. The crystal of Curve 1 was the one measured in the spin-flop experiments. It is interesting to note that the transition occurs over a broad temperature range for all crystals containing Ti. The transition tempera-

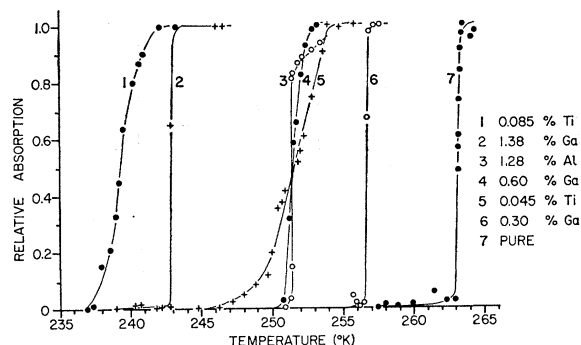


Fig. 6. The relative peak height of the magnetic-resonance absorption line versus the absolute temperature.

ture, defined as the temperature at which the magnetization is half the room-temperature value, is listed for each doping under the heading "Magnet." in Table I. The agreement with the theoretical values is remarkably good and hence provides substantial support for the model proposed for the origin of the anisotropy.

The transition was also studied with neutron diffraction by observing the 111 reflection, which is wholly magnetic. The intensity of this reflection depends on the angle  $\theta$  that the sublattice magnetizations make with the  $[111]$  direction, being a maximum for  $\theta = \frac{1}{2}\pi$  and zero for  $\theta = 0$ . Curves of the peak intensity of the 111 line, plotted as a function of temperature, have been published earlier elsewhere.<sup>2,6</sup> One such curve was for the crystal of Curve 4 in Fig. 5 (shown as Curve 3, Fig. 2 in Morrish, Johnston, and Curry<sup>2</sup>); the curves obtained by the two different techniques were very similar. In general, the magnetization and neutron-diffraction measurements were made on different samples; frequently, however, they had been cut from the same large crystal. The transition temperature, defined as the temperature at which the peak intensity of the 111 line was half its room-temperature value, is listed under the heading "Neut. diff." in Table I. Because of secondary extinction, known to be appreciable in these highly perfect crystals, this definition may lead to transition temperatures that are slightly different from the ones for the magnetization measurements. In addition, of course, there may be small differences in the dopings of the crystals. Nevertheless, the agreement between the neutron-diffraction and magnetization measurements is reasonably good, the greatest discrepancies being for the highest Al and Ga dopings and all the Ti dopings.

Finally, the transition was investigated by measuring the magnetic-resonance absorption line as a function of temperature. Since the observed mode of oscillation is essentially a precession of the weak ferromagnetic moment, the resonance spectrum will disappear when the small spontaneous magnetization disappears. The experiments were conducted at  $K$ -band frequencies with spherical samples of about 1-mm diam. The peak height of the absorption line relative to the room-tempera-

ture value is shown as a function of temperature for a number of dopings in Fig. 6. The transitions tend to be sharper than in the magnetization or neutron-diffraction work; actually, about 90% of some transitions were completed within a temperature of 0.1°C. The transition temperature, defined as the temperature at which the line height was half the room-temperature value, is listed under the heading "Reson." in Table I. The application of a static magnetic field of approximately 2000 Oe, required in order to observe the resonance, may have produced a small shift in the transition temperature.<sup>16</sup> However, the agreement with the other experimental measurements is again respectable, the greatest deviations being for the Ti-doped samples.

The above discrepancies and transition widths can be understood if it is assumed that the doping is inhomogeneous,<sup>17</sup> particularly for the Ti and the most heavily doped crystals. If the spins in various regions of the crystal were either parallel or perpendicular to the trigonal axis, depending on the local concentration of impurity cations, the end effect would be to broaden the transition for an entire crystal.<sup>18</sup> Additional evidence for a variation in the impurity concentration was obtained from the resonance experiments. For some of the small spheres with narrow transitions, the absorption was not a continuous function of temperature, but took place in a small number of discrete steps. Finally, further evidence that the discrepancies in the data are due to inhomogeneities was found by remeasuring all the Ti-doped crystals used in the neutron-diffraction experiments with the magnetization method. The transition temperature obtained by the two techniques for each specimen then agreed within 1°C.

In the flux technique of growing crystals, too viscous a melt tends to produce inhomogeneously doped crystals. The question arises as to why the Ti distribution is more nonuniform than that of the other cations. Ilmenite ( $\text{FeTiO}_3$ ) belongs to the same space group as hematite. However, the Fe and Ti ions lie in alternate (111) layers; that is, a plane contains either Fe or Ti but not both. Hence, in Ti-doped crystals, there may be a tendency for Ti ions to concentrate together in particular layers in certain parts of the crystal. Such an inclination would of course be conducive to the production of inhomogeneities. Al and Ga ions apparently do not tend to order in separate layers. Another difference that may be significant is that Ti is added as  $\text{TiO}_2$  in the Pt crucible, whereas Al and Ga are introduced in the form of  $\text{Al}_2\text{O}_3$  and  $\text{Ga}_2\text{O}_3$ . It is also reasonable to expect that for all impurity cations, the inhomogeneity would be greater the heavier the doping, and the data appear to bear this out.

<sup>16</sup> J. Kaczér and T. Shalnikova, in *Proceedings of the International Conference on Magnetism, Nottingham, 1964* (Institute of Physics and the Physical Society, London, 1964), p. 589.

<sup>17</sup> P. J. Flanders and J. P. Remeika, *Phil. Mag.* **11**, 1271 (1965).

<sup>18</sup> P. Imbert and A. Gerard, *Compt. Rend.* **257**, 1054 (1963).

## BASAL-PLANE ANISOTROPY

The anisotropy in the basal plane can be conveniently studied by observing the magnetic-resonance spectra. To see this, first consider the expression for the in-plane anisotropy:

$$F_{K_3''} = K_3'' \sin^6 \theta \cos 6 \varphi \\ = \frac{1}{2} K_3'' (\sin^6 \theta_A \cos 6 \varphi_A' + \sin^6 \theta_B \cos 6 \varphi_B');$$

here  $\theta_A$  and  $\theta_B$  are the angles the magnetization of the  $A$  and  $B$  sublattices make with the  $[111]$  axis, and  $\varphi_A'$  and  $\varphi_B'$  are the azimuthal angles the magnetization of the  $A$  and  $B$  sublattices make with a crystallographic axis, say  $a_1$ , respectively. It is useful to rewrite this expression in terms of the angle  $\beta$  between the direction of the applied field (in the basal plane) and the same crystallographic  $a_1$  axis, namely,

$$F_{K_3''} = \frac{1}{2} K_3'' [\sin^6 \theta_A \cos 6(\varphi_A + \beta) + \sin^6 \theta_B \cos 6(\varphi_B + \beta)] \\ = \frac{1}{2} K_3'' [\cos 6\beta (\sin^6 \theta_A \cos 6 \varphi_A + \sin^6 \theta_B \cos 6 \varphi_B) \\ - \sin 6\beta (\sin^6 \theta_A \sin 6 \varphi_A + \sin^6 \theta_B \cos 6 \varphi_B)],$$

where now  $\varphi_A$  and  $\varphi_B$  are the azimuthal angles between the  $A$  and  $B$  sublattice magnetizations and the direction of the applied field. Since the canting arising from the Dzialoshinski-Moriya interaction is very small, it follows that, to a good order of approximation,

$$F_{K_3''} = \frac{1}{2} K_3'' \cos 6\beta (\sin^6 \theta_A \cos 6 \varphi_A + \sin^6 \theta_B \cos 6 \varphi_B). \quad (9)$$

The total free energy of the system then becomes

$$F_T = -\mathbf{M}_A \cdot \mathbf{H} - \mathbf{M}_B \cdot \mathbf{H} + N_{AB} \mathbf{M}_A \cdot \mathbf{M}_B - \mathfrak{D} \cdot (\mathbf{M}_A \times \mathbf{M}_B) \\ + \frac{1}{2} K_1' (\sin^2 \theta_A + \sin^2 \theta_B) + \frac{1}{2} K_2' (\sin^4 \theta_A + \sin^4 \theta_B) \\ + \frac{1}{2} K_3' (\sin^6 \theta_A + \sin^6 \theta_B) \\ + \frac{1}{2} K_3'' \cos 6\beta (\sin^6 \theta_A \cos 6 \varphi_A + \sin^6 \theta_B \cos 6 \varphi_B) \\ + F_{me}(\theta_A, \theta_B, \varphi_A, \varphi_B, \zeta), \quad (10)$$

where  $\mathfrak{D}$  is the Dzialoshinski-Moriya vector and lies along the  $[111]$  direction,  $F_{me}$  is the magnetoelastic term, and  $\zeta$  represents the lattice distortion.

Next, the resonance equations of the system for small oscillations about the equilibrium position are given, in general, by

$$\begin{vmatrix} F_{T\theta_A\theta_A} & F_{T\theta_A\theta_B} & F_{T\theta_A\varphi_A} + \frac{i\omega_r M_A}{\gamma} \sin\theta_A & F_{T\theta_A\varphi_B} \\ F_{T\theta_A\theta_B} & F_{T\theta_B\theta_B} & F_{T\theta_B\varphi_A} & F_{T\theta_B\varphi_B} + \frac{i\omega_r M_B}{\gamma} \sin\theta_B \\ F_{T\theta_A\varphi_A} - \frac{i\omega_r M_A}{\gamma} \sin\theta_A & F_{T\theta_B\varphi_A} & F_{T\varphi_A\varphi_A} & F_{T\varphi_A\varphi_B} \\ F_{T\theta_A\varphi_B} & F_{T\theta_B\varphi_B} - \frac{i\omega_r M_B}{\gamma} \sin\theta_B & F_{T\varphi_A\varphi_B} & F_{T\varphi_B\varphi_B} \end{vmatrix} = 0, \quad (11)$$

where

$$F_{T\theta_A\theta_A} = \frac{\partial^2 F_T}{\partial \theta_A^2}, \quad F_{T\theta_A\theta_B} = \frac{\partial^2 F_T}{\partial \theta_A \partial \theta_B}, \\ F_{T\theta_A\varphi_A} = \frac{\partial^2 F_T}{\partial \theta_A \partial \varphi_A}, \quad \text{etc.},$$

are evaluated at the static equilibrium position and  $\gamma = ge/2mc$ .

Application of Eq. (11) to Eq. (10) then leads to two resonance conditions. One is a high-frequency mode that was not observed in our experiments. The other is given by

$$\left(\frac{\omega_r}{\gamma}\right)^2 = H_r(H_r + H_{\mathfrak{D}}) + 2H_m H_{K_3''} \cos 6\beta + 2H_m H_{me}, \quad (12)$$

where  $H_r$  is the applied field required for resonance for the angular frequency  $\omega_r$ ,  $H_{\mathfrak{D}} = |\mathfrak{D}|M$ ,  $H_{K_3''} = 18K_3''/M$ ,  $M = |M_i|$ ,  $i = A, B$ , and  $H_{me}$  is the equivalent magnetoelastic field, assumed to be essentially

constant. Others<sup>19,20</sup> have recognized this result by generalizing an equation derived earlier by Pincus.<sup>8</sup> Clearly, the reason the basal plane can be studied conveniently with resonance techniques is that  $H_{K_3''} \cos \beta$  is multiplied by the molecular field  $H_m$ , which is a large number.

The angular variation observed for the resonance field  $H_r$  with respect to the crystallographic axes in the basal plane is indicated schematically in Fig. 7. It follows immediately that the easy direction for the weak spontaneous moment lies in a glide plane, whereas the easy direction for the sublattice magnetizations,  $M_A$  and  $M_B$ , coincides with the  $a_1$ ,  $a_2$ , and  $a_3$  axes. These results are in agreement with recent findings.<sup>19,21</sup> The magnitude of the resonance field  $H_r$  for a pure sample is plotted as a function of  $\phi$ , the angle between the applied

<sup>19</sup> A. Tasaki and S. Iida, J. Phys. Soc. Japan 18, 1148 (1963).

<sup>20</sup> A. H. Morrish and C. W. Searle, in *Proceedings of the International Conference on Magnetism, Nottingham, 1964* (Institute of Physics and the Physical Society, London, 1964), p. 574.

<sup>21</sup> R. O. Keeling and R. E. Schramm, Bull. Am. Phys. Soc. 11, 378 (1966).

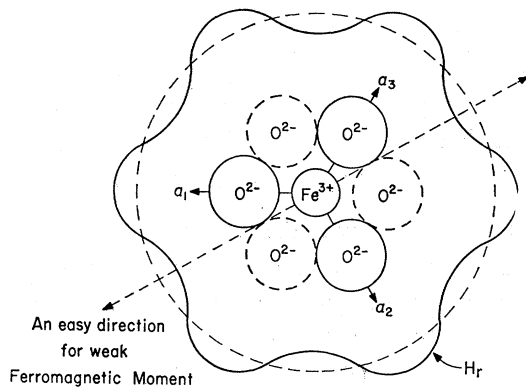


FIG. 7. Schematic variation of the resonance field  $H_r$  with respect to the crystal structure of hematite. The basal plane is that of the page and the hexagonal axes  $a_1$ ,  $a_2$ , and  $a_3$  are indicated. The intersection of the glide plane with the (111) plane is shown as the dashed straight line, and coincides with the easy direction for the small spontaneous magnetization. The  $O^{2-}$  ions represented by the solid and dashed circles lie above and below the  $Fe^{3+}$  ion.

field and an arbitrary axis in the basal plane in Fig. 8 (curve A). If the value of  $H_m = 1.04 \times 10^7$  Oe is used, the data yield  $|H_{K_3''}| = 1.1 \times 10^{-2}$  Oe. The basal-plane anisotropy for several of the doped samples was also investigated. The magnitude of  $H_{K_3''}$  was found to be less by from 10% to 35%, but did not depend in a consistent way on the kind and amount of the impurity ions. For example, it was observed that for a sample with 1.28 mole % Al,  $|H_{K_3''}| = 1.0 \times 10^{-2}$  Oe, for 1.38 mole % Ga,  $|H_{K_3''}| = 0.7 \times 10^{-2}$  Oe, and for either 0.081 or 0.17 mole % Ti,  $|H_{K_3''}| = 0.8 \times 10^{-2}$  Oe. The error in determining  $H_{K_3''}$ , however, is large. Hence the only reliable conclusion to be made is that the in-plane anisotropy is relatively insensitive to doping, the effect being to reduce somewhat  $|H_{K_3''}|$ .

On the other hand, the in-plane anisotropy was found to be sensitive to stress. To illustrate, the sample was mounted in the microwave cavity with a slow-drying glue. The initial variation of the resonance field with angle is shown as curve A in Fig. 8. Curve B was obtained 1 h later and curve C 1 day later. The hardening of the glue presumably introduced both compression and shear strains. Further, since the symmetry is lost, at least part of the stress must have been distributed nonuniformly. If uniform stresses are appropriately applied, a trigonal symmetry with a much larger effective  $|H_{K_3''}|$  would be observed. The anomalously large

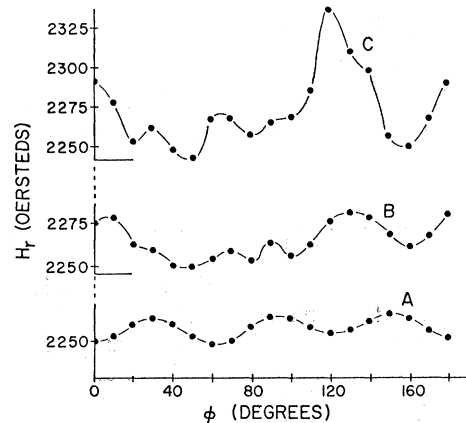


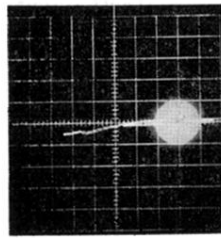
FIG. 8. To illustrate the effect of nonuniform stresses on the basal-plane anisotropy of pure hematite. Here  $H_r$  is the field applied in the (111) plane required for magnetic resonance and  $\phi$  is the angle between  $H_r$  and an arbitrary direction in the basal plane. The hematite crystal was immersed in a slow-drying glue. Curve A was obtained initially, curve B after 1 h, and curve C after 1 day.

value of  $|K_3''|$  obtained in some static experiments<sup>22</sup> may have its origin in symmetric internal strains.

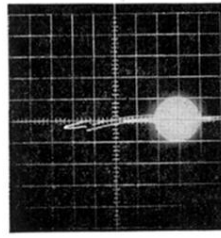
Thus there appear to be three significant results concerning the basal-plane anisotropy, viz., (1) it possesses the same symmetry as the lattice, (2) it is relatively unaffected by the presence of foreign cations including  $Fe^{2+}$ , and (3) it is extremely dependent on stresses. These findings suggest that the crystalline anisotropy in the basal plane should be considered to originate from a variation of the magnetoelastic coupling.

*Note added in proof.* An electron-beam microprobe analysis of two doped hematite crystals has been made recently. In a scan over the (111) face of the sample doped with 0.170 mole % Ti, the titanium content was found to vary by about 50% over a distance of 2 mm. However, the curve of the Ti content versus linear coordinate was continuous. For the sample with 1.38 mole % Ga (the one of curve 4 in Fig. 5), the gallium concentration appeared to be uniform except at some localized regions where it suddenly became much higher. Visual inspection along the scan path showed areas that may be inclusions of different crystal phases. Hence these results support the conjectures made in the paper concerning the inhomogeneous doping and crystal-structure effects.

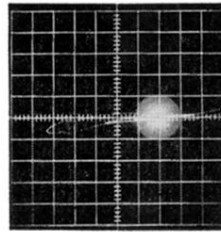
<sup>22</sup> P. J. Flanders and W. J. Schuele, *Phil. Mag.* **9**, 485 (1964).



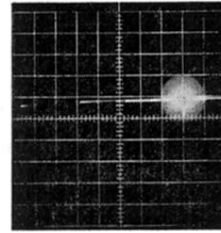
(a)  
T = 77 °K Pure



(b)  
T = 77 °K 0.83 mole % Al

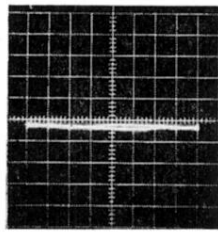


(c)  
T = 77 °K 0.045 mole % Ti

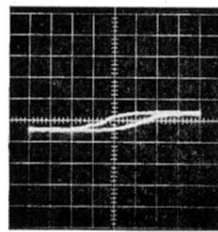


(d)  
T = 258 °K Pure

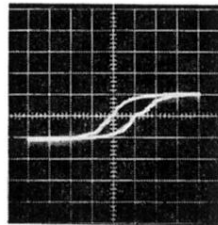
FIG. 1. Spin-flop transitions in pure and doped hematite crystals. (a)  $H_{sf} = 67.8$  kOe, (b)  $H_{sf} = 64.0$  kOe, (c)  $H_{sf} = 64.6$  kOe, and (d)  $H_{sf} = 26.2$  kOe.



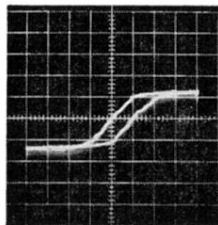
(a) T=262.7 °K



(b) T=263.4 °K



(c) T=263.7 °K



(d) T=264.0 °K

FIG. 4. The low-temperature (Morin) transition for pure hematite detected via the temperature variation of the  $M$ - $H$  loop of the weak ferromagnetic moment.